scientific data

OPEN

DATA DESCRIPTOR

Proteomic Data and Drug Implications for Cerebral Microvascular Endothelial Cells Under Varying Oxygen Levels

Sarah Barakat[1]✉, Fan Yang[2], Hayriye Ecem Yelkenci[1], Kıvanç Kök[1,3]✉, Giovanni E. Mann[2] & Emrah Eroğlu[1,4]

Hyperoxia in standard cell cultures (18 kPa O_2) imposes cellular oxidative stress, potentially skewing research and drug screening outcomes. Cerebral microvascular endothelial cells (hCMEC/D3) experience no more than 7 kPa O_2 *in vivo*. In this study, hCMEC/D3 cells were adapted to 5 kPa O_2 for 5 days to optimize an *in vitro* physiological cell culture model. Using a SYNAPT G2-Si mass spectrometer, we compared the proteomic profiles of cells cultured under 5 kPa versus 18 kPa O_2. A substantial proteomic shift under hyperoxia highlighted the strong impact of oxygen levels on protein expression. We further investigated the effect of oxygen levels on drug screening using sulforaphane (SFN), an inducer of NRF2-regulated antioxidant defense genes. SFN induced more pronounced changes in proteomic profiles under 18 kPa O_2 compared to 5 kPa, indicating oxygen-dependent cellular drug responses. This dataset offers a valuable resource for analyzing oxygen-sensitive proteomic changes. Comparative studies using different drugs or cell types could further elucidate oxygen-dependent signaling and inform the development of therapies aligned with physiological oxygen levels.

Background & Summary

Oxygen is fundamental to cellular function, driving metabolic processes and energy production. Cellular oxygen levels are finely adapted across tissues, determined by their specific physiological demands[1]. Recent studies using various cell types have demonstrated that different oxygen levels considerably impact cellular behavior and function[1]. For example, memory CD8 + T cells cultured under their physiologically normoxic oxygen (3 kPa), rather than standard cell culture atmospheric oxygen levels (~18 kPa), shift metabolism to glycolysis and enhance their immune responses[2]. Likewise, neurons and astrocytes cultured under 5 kPa oxygen display increased glycolytic activity[3]. In breast cancer cells, exposure to atmospheric oxygen levels influences the expression and activity of drug targets, thus increasing drug sensitivity[4]. Furthermore, oxygen levels have been shown to regulate translation mechanisms, such as through distinct cap-binding proteins, which in turn shape the proteome composition and impact cellular function[5].

Despite the critical role of oxygen in cellular function, most *in vitro* studies are conducted under atmospheric oxygen levels (~18 kPa), which do not accurately reflect the lower oxygen tensions encountered by cells *in vivo*, thereby limiting the physiological relevance of such studies[1,6]. Endothelial cells regulate oxygen and nutrient transport, making their response to oxygen levels critical[1]. Pulmonary endothelial cells, for example, have been shown to alter their surface glycosylation under hyperoxia affecting cellular signaling and interactions[7]. Notably, umbilical vein endothelial cells respond to reduced oxygen levels by modifying key cellular functions, including cytoskeletal remodeling and ER stress[8]. The brain, with its high metabolic demands, is particularly sensitive to

[1]Regenerative and Restorative Medicine Research Center (REMER), Research Institute for Health Sciences and Technologies (SABITA), Istanbul Medipol University, Istanbul, 34810, Turkey. [2]King's British Heart Foundation Centre of Research Excellence, School of Cardiovascular and Metabolic Medicine & Sciences, Faculty of Life Sciences & Medicine, King's College London, 150 Stamford Street, London, SE1 9NH, UK. [3]Department of Biostatistics and Medical Informatics, International School of Medicine, Istanbul Medipol University, Istanbul, 34810, Turkey. [4]Molecular Biology, Genetics, and Bioengineering Program, Faculty of Engineering and Natural Sciences, Sabanci University, Istanbul, 34956, Turkey. ✉e-mail: sarah.barakat1@medipol.edu.tr; guvanch@medipol.edu.tr

oxygen supply[9]. Brain vascular endothelial cells lining the blood-brain barrier[10] typically function under lower oxygen tensions, around 3–7 kPa[1], and precise regulation is critical to obviate oxidative stress, inflammation, and cellular dysfunction[11,12]. Our previous studies demonstrated that hCMEC/D3 cells exhibit distinct antioxidant responses under varying oxygen levels, as well as differential sensitivity to commonly used drugs known to induce cellular antioxidant properties[13,14]. Furthermore, pericellular oxygen levels influence cellular iron uptake, thereby affecting nitric oxide bioavailability[15]. Optimizing oxygen levels in experimental conditions is therefore crucial, particularly in contexts such as stroke research, where *in vitro* models of oxygen and glucose deprivation are often compared to controls incubated under conventional atmospheric oxygen levels, which may not accurately mimic the physiological microenvironment[16].

In this study, we explored the impact of oxygen levels on the proteomic profile of oxygen-sensitive brain endothelial cells, utilizing hCMEC/D3 cells as a representative model. Through a comparative analysis of proteomic profiles under hyperoxic (18 kPa O_2) and physiologically normoxic (5 kPa O_2) conditions, we uncovered a protein expression signature distinguishing the two respective sample groups. Given the role of oxygen tension in endothelial function, we further investigated how these levels influence cellular responses to drug treatment, using sulforaphane (SFN) as a known activator of the transcription factor NRF2, involved in cellular oxidative stress defenses[17]. This comparison enabled us to evaluate the effectiveness of SFN under *in vivo*-like oxygen conditions to provide insights into the broader impact of oxygen tension on drug efficacy. The availability of this proteomic dataset provides a valuable resource for analyzing oxygen-sensitive pathways, enabling researchers to compare data across cell types to identify universal and cell-specific responses. It can also be integrated with transcriptomic, metabolomic, or epigenomic datasets to gain a more comprehensive insight into the mechanisms by which pericellular oxygen affects cellular function. Additionally, this dataset allows for the comparison of other drug effects under different oxygen levels, facilitating the development of more physiologically relevant drug screening tools[14,15] and protocols to inform the design and interpretation of therapeutic interventions in both health and disease.

Methods

hCMEC/D3 cell culture conditions. hCMEC/D3 cells (obtained from Tebubio, UK) were cultured in 1% rat-tail collagen I coated substrates (Sigma) in EBM phenol-red free basal cell media (Lonza) supplemented with EGM-2MV growth factors 0.025% (v/v) rhEGF, 0.025% (v/v) VEGF, 0.025% (v/v) IGF, 0.1% (v/v) rhFGF, 0.1% (v/v) ascorbic acid, 0.04% (v/v) hydrocortisone, 2.5% fetal bovine serum (FBS) (Lonza) and 1% penicillin (100U/ml)/ streptomycin (100 µg/ml). Culture media were pre-equilibrated under either ambient air (18 kPa O_2) or 5 kPa O_2 in a dual Scitive Workstation (Baker, USA) prior to experimentation. hCMEC/D3 cells monolayers were maintained for at least 5 days in the O_2-controlled workstation, gassed to 18 kPa or 5 kPa O_2 under 5% CO_2 at 37 °C to establish an oxygen and redox phenotype in the absence of HIF1-α stabilization[18]. Experiments with hCMEC/D3 cells were performed at passages 27–34 (recommended range for maintaining endothelial phenotype and function[19,20]) within the O_2-controlled workstation for long-term adaptation of cells to a defined O_2 level to prevent re-exposure of cells adapted to 5 kPa O_2 to atmospheric oxygen.

Experimental design of proteomics experiment. hCMEC/D3 cells were collected after adaptation of cells for 5 days to 18 or 5 kPa O_2. hCMEC/D3 cells adapted to 18 or 5 kPa O_2 were also treated for 24 h with vehicle (veh, 0.01% dimethyl sulfoxide (DMSO) (Sigma-Aldrich, UK) or sulforaphane (SFN, 2.5 µM, Sigma-Aldrich, UK), respectively. Cell pellets were washed twice with PBS and stored at −80 °C. All experiments were repeated in 3 independent cultures.

Sample preparation for liquid chromatography mass spectrometry (lc-ms/ms). Cells were lysed for total protein extraction using a protein extraction kit (ab270054, abcam) following the standard protocol[21]. Cells were lysed by resuspending cells in a lysis buffer with protease inhibitors cocktail (ab270061, Expedeon, Heidelberg, Germany), then boiled at 100 °C for 10 min. After cooling for 1 h at 4 °C, the samples were centrifuged at 16,000 g for 20 min at 4 °C, and supernatants were collected. Protein concentration was determined using a Qubit 3.0 Fluorometer (Q33216, Invitrogen, Life Technologies Corporation, Carlsbad, CA, USA). Proteins were digested using the FASP method[21] (ab270519, Abcam, Cambridge, UK), where 50 µg of protein were collected on 30 kDa cut-off spin column with 6 M urea, alkylated with 10 mM iodoacetamide at room temperature for 20 min in the dark, then finally digested overnight with a 1:100 ratio MS grade trypsin protease (90057, Thermo Fisher Scientific, Waltham, MA, USA) at 37 °C. Peptides were eluted, lyophilized, and reconstituted in 0.1% formic acid (1002642510, Merck) at a concentration of 100 ng/µL for LC-MS/MS analysis.

Liquid chromatography mass spectrometry analysis. Proteomic analysis was performed using an ACQUITY UPLC M-Class system coupled to a SYNAPT G2-Si high-definition mass spectrometer (Waters, Milford, MA, USA) for untargeted proteomics, following a published protocol[22]. For this, both the analytical column (ACQUITY UPLC M-Class HSS T3, 100 Å, 75 µm × 250 mm, 1.8 µm, 186007474, Waters) and the trap column (ACQUITY UPLC M-Class Symmetry C18, 180 µm × 20 mm, 186007496, Waters) were equilibrated with 97% mobile phase A (0.1% formic acid in LC-MS grade water). The column temperature was maintained at 55 °C. Peptides were initially trapped on the trap column and subsequently eluted onto the analytical column using a 90-minute gradient of mobile phase B (0.1% formic acid in acetonitrile, 100,029, Merck) from 4% to 40% at a flow rate of 0.3 µL/min.

Data were acquired in positive ion mode with a resolution mode setting and a 0.6-second cycle time. A data-independent acquisition (DIA) approach was utilized, covering an m/z range of 50–1900, with ion mobility separation (IMS) enhancing the separation of ions in the gas phase. Low and high collision energies were set to 10 V and 30 V, respectively, with wave velocities ramped from 1000 to 55 m/s across the IMS cycle. The trap

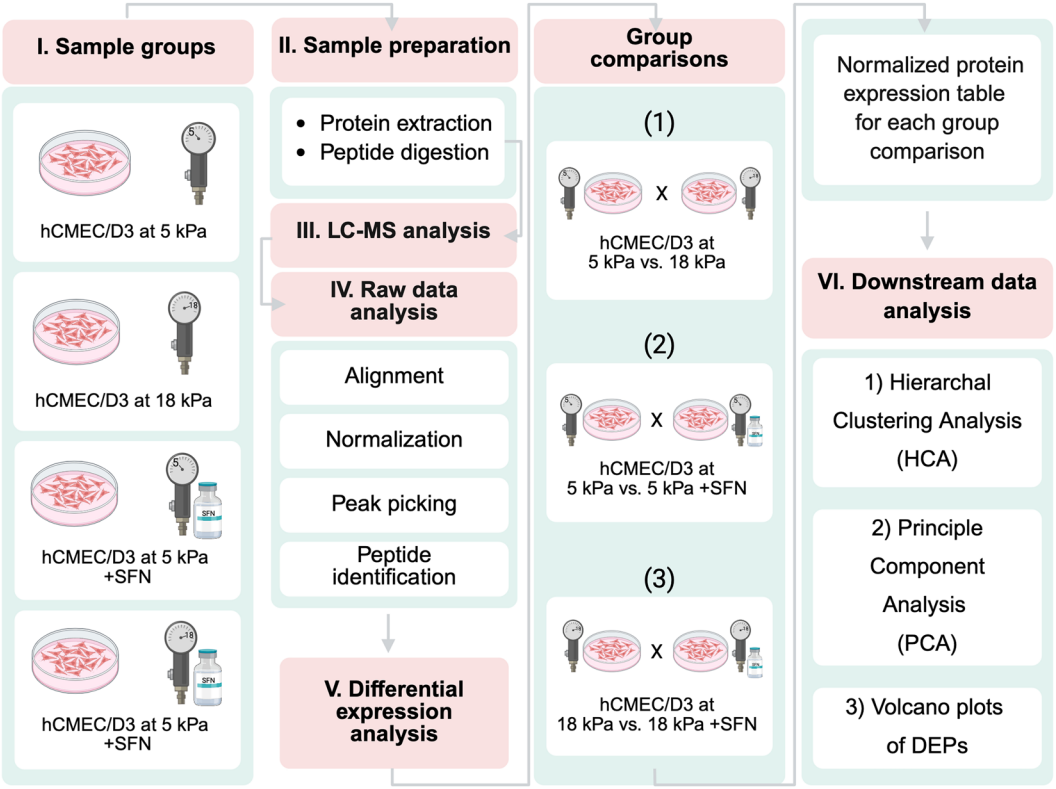

Fig. 1 Workflow of Proteomics Experiment: Experimental design and data analysis.

release time was 500 μs, with a trap height of 15 V, and the IMS wave delay was set to 1000 μs. To ensure mass accuracy and stability, 100 fmol/μL Glu-1-fibrinopeptide B (186,007,091–2, Waters MA, USA) was used for lock mass calibration, introduced at 45-second intervals.

Data Records

The raw mass spectrometry data and the normalized protein expression dataset along with the extended metadata table have been deposited in the jPOST repository[23] under ID JPST003477[24] and accessible in ProteomeXchange[25] under ID PXD060622[26]. The deposited files include the following main types:

- Compressed raw data files (xxx.raw.zip): Contain the original mass spectrometry data, with each sample deposited in a separate file.
- Detected protein files (xxx.csv): Contain the detected proteins, as identified by Progenesis QI for Proteomics software, with each sample deposited in a separate file.
- Combined expression dataset Excel file (combined_expression_dataset_with_all_samples.xlsx): this Excel file contains the final results from Progenesis QI for Proteomics software. It includes the following information: UniProt accession IDs, peptide count, unique peptides, confidence scores, ANOVA p-values, protein description, and normalized abundances for all detected proteins. The overall dataset sheet includes information for all samples while separate sheets provide information for each group comparison.
- Extended metadata Excel file (Metadata_of_Proteomics_Analysis.xlsx): Provides a Table of comprehensive information about the proteomics analysis. It includes the sample category, which describes the oxygen levels (5 kPa and 18 kPa), and the sample subcategory, detailing the SFN treatment groups within each oxygen level (−/+ SFN). The Table also includes information on replicates, specifying the number of independent biological replicates (represented by the first number in the nomenclature) and the number of technical replicates per biological replicate (represented by the second number). For example, "18 kPa_3_2" indicates the second technical replicate of the third biological replicate for a sample cultured at an oxygen level of 18 kPa. It includes sample IDs, which correspond to the labels for the samples used in figures, divided into IDs for non-averaged (individual data points) and averaged (mean values) results. The repository IDs provide references to the IDs of samples as stored in the data submission repository. Lastly, the total sample count represents the total number of samples for each experimental condition, encompassing both biological and technical replicates. A detailed description of the proteomics workflow and data analysis is provided in Fig. 1, while the metadata of the presented dataset is provided in Table 1.

Sample category	Sample subcategory	Biological replicate ID	Technical replicate ID	ID in figures		Total sample count
				Non-averaged	Averaged	
5 kPa	(−) SFN	1	1	5 kPa_1_1	5 kPa_1	9
			2	5 kPa_1_2		
			3	5 kPa_1_3		
		2	1	5 kPa_2_1	5 kPa_2	
			2	5 kPa_2_2		
			3	5 kPa_2_3		
		3	1	5 kPa_3_1	5 kPa_3	
			2	5 kPa_3_2		
			3	5 kPa_3_3		
	(+) SFN	1	1	5 kPa_1 + SFN	—	3
			2	5 kPa_2 + SFN	—	
			3	5 kPa_3 + SFN	—	
18 kPa	(−) SFN	1	1	18 kPa_1_1	18 kPa_1	9
			2	18 kPa_1_2		
			3	18 kPa_1_3		
		2	1	18 kPa_2_1	18 kPa_2	
			2	18 kPa_2_2		
			3	18 kPa_2_3		
		3	1	18 kPa_3_1	18 kPa_3	
			2	18 kPa_3_2		
			3	18 kPa_3_3		
	(+) SFN	1	1	18 kPa_1 + SFN	—	3
			2	18 kPa_2 + SFN	—	
			3	18 kPa_3 + SFN	—	

Table 1. *Metadata of the proteomic profiling dataset* of hCMEC/D3 cells exposed to varying oxygen levels (5 kPa and 18 kPa) in the absence or presence of SFN.

Technical Validation

Quality evaluation of mass spectrometry data. To evaluate the quality of our mass spectrometry data, we assessed mass accuracy, precursor ion m/z values, charge state distribution, missed cleavage frequency, and peptide ion abundance across experimental conditions. The mass errors of identified peptide ions were centered around zero and predominantly fell within ± 2 standard deviations from the mean, indicating high mass accuracy and proper instrument calibration (Fig. 2a). The majority of precursor ions fell within the 500–1000 m/z range, consistent with efficient detection of tryptic peptides (Fig. 2b). Most peptides carried charge states of + 2 or + 3, which are favorable for fragmentation and reliable identification in tandem MS (Fig. 2c). Over 80% of the peptides had no missed cleavages, and very few exceeded one missed cleavage, confirming high enzymatic digestion efficiency (Fig. 2d). To assess identification performance, we analyzed the percentage of normalized abundance of peptide ions under each experimental condition. In all conditions (18 kPa, 5 kPa, 18 kPa + SFN, and 5 kPa + SFN) identified peptides spanned a broad abundance range with no pronounced skew toward high-intensity ions, indicating effective quantification and minimal saturation bias (Fig. 2e–h).

Mass spectrometry raw data analysis. Peptide identification and quantification were conducted using Progenesis-QI for Proteomics software (Waters, https://www.nonlinear.com/progenesis/qi-for-proteomics/), using the UniProt Human database (accessed on 11 November 2024) and the MS search-based peptide identification method. We followed previously published protocols[22]. Key parameters included a low energy threshold of 200 counts, a high energy threshold of 50 counts, and an intensity threshold of 750 counts. For alignment, the most suitable run was selected, and normalization was performed using the "normalize to all peptide ions" option. Additional analysis settings included a maximum charge of 5, allowance for one missed cleavage, fixed carbamidomethylation, variable methionine oxidation, and a maximum protein mass of 400 kDa. Ion matching requirements were set to ≥3 fragments per peptide, ≥7 fragments per protein, and ≥1 peptide per protein. Statistical analysis between comparison groups was performed in Progenesis-QI for Proteomics using one-way ANOVA functionality. Here, an Independent Student's t-test was applied to compute p-values, resulting in an output file showing identified proteins with their abundance levels and obtained p-values. The resulting data were then filtered to exclude all proteins with ≤2 unique peptides. After filtering, the total number of identified proteins for the 18 kPa vs. 5 kPa comparison was 2,182, while 2,183 proteins were identified for the 5 kPa vs. 5 kPa + SFN comparison, and 2,185 for the 18 kPa vs. 18 kPa + SFN comparison. These proteins were exported to Babelomics 5[27,28] (http://babelomics.bioinfo.cipf.es/) for further analysis, where multiple test correction (MTC) was applied using the Benjamini and Hochberg method, with an adjusted p-value threshold of 0.05. Due to the limited number of replicates (only 3 technical replicates per SFN-treated sample), no significant proteins ($p < 0.05$) were detected after MTC for the SFN-treated samples in comparison to controls at both 5 kPa and

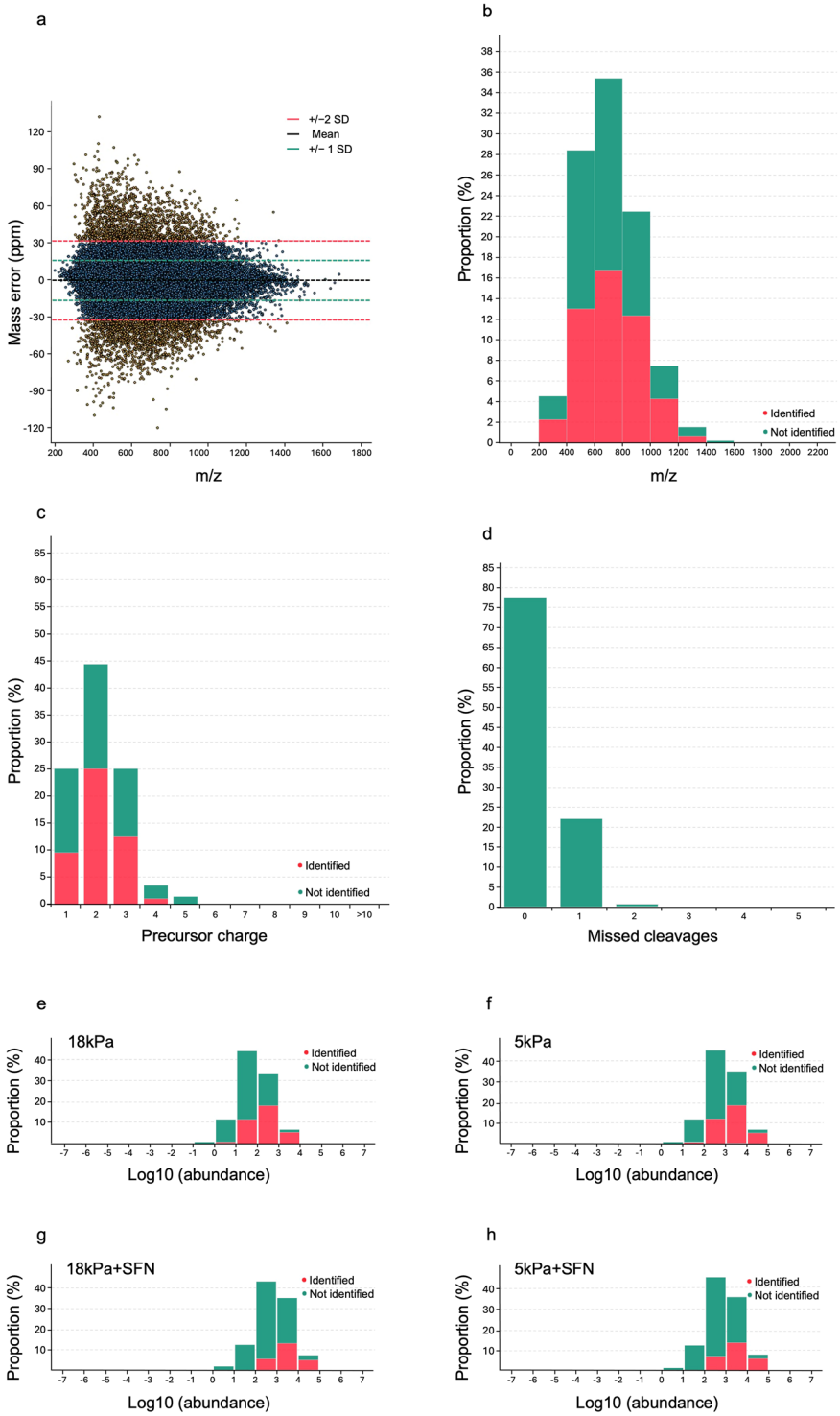

Fig. 2 Quality Evaluation of Mass Spectrometry Data. (**a**) Mass accuracy of identified peptide ions. (**b**) Distribution of m/z values for all precursor ions. (**c**) Percentage of precursor ions with various charge states. (**d**) Distribution of missed cleavages per identified peptide ion. (**e–h**) Abundance distribution of peptide ions in each condition (18 kPa, 5 kPa, 18 kPa + SFN, 5 kPa + SFN, respectively), shown as log10 of normalized abundance.

18 kPa. Therefore, we retained the data prior to MTC for these two comparisons. However, for the 18 kPa vs. 5 kPa comparison (without SFN treatment), which had a total of 9 replicates per condition (3 biological replicates, each with 3 technical replicates), significant proteins (adj. $p < 0.05$) were still identified after MTC. Fold changes were calculated in Babelomics 5 with a cutoff set at 1.4. This generated a final spreadsheet listing all identified proteins along with their respective abundances, significance test results, and fold changes, which was used for downstream analysis.

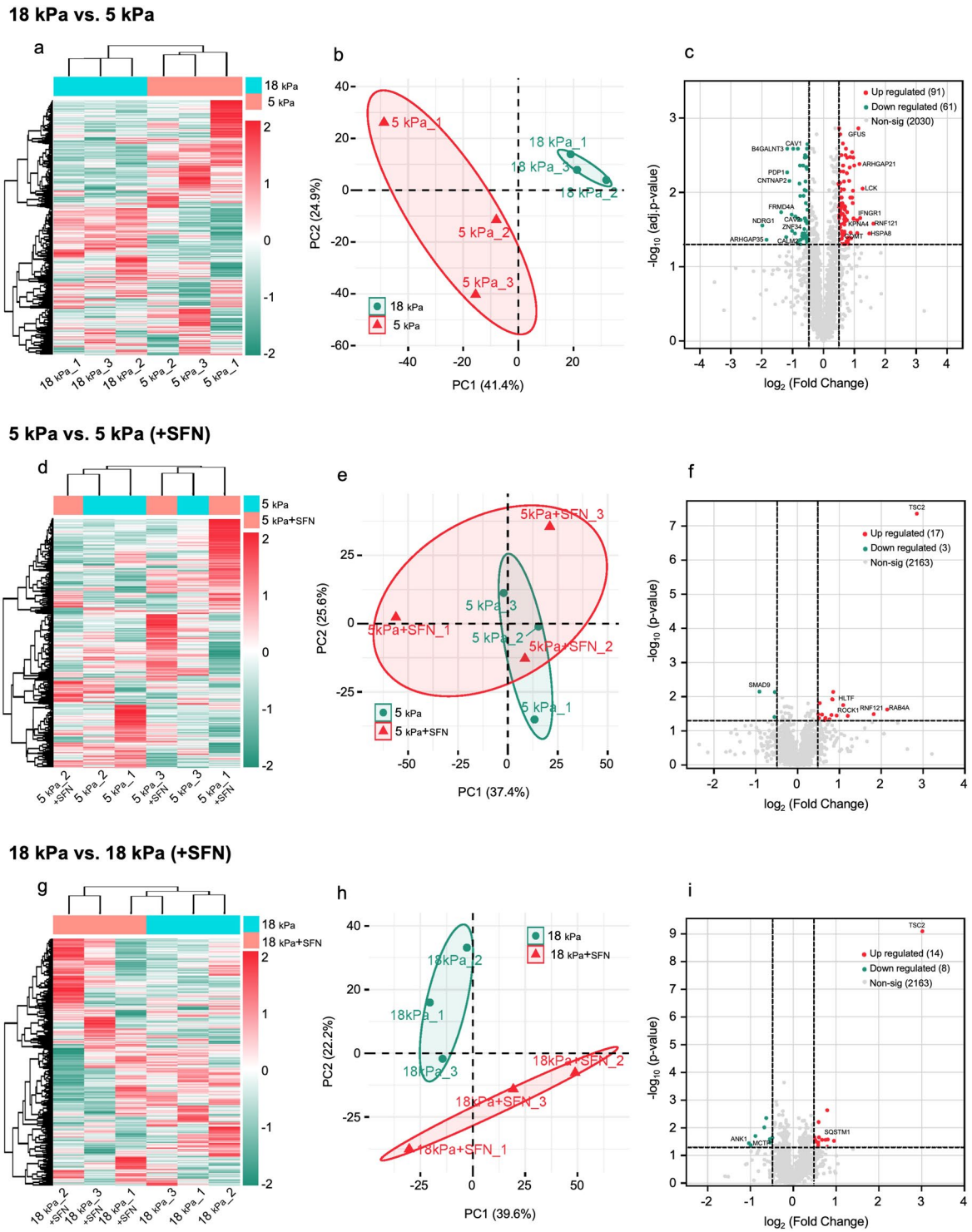

Fig. 3 Differential Protein Expression Analysis of hCMEC/D3 Cells Cultured under 5 kPa vs. 18 kPa O_2 in the Absence or Presence of SFN. (**a,d,g**) Hierarchical clustering heatmap analysis of total identified proteins, showing clustering of samples according to: (**a**) Oxygen levels: 5 kPa vs. 18 kPa, (**d**) SFN treatment at 5 kPa, **g**) SFN treatment at 18 kPa. The color scale represents protein expression levels, with ■ indicating downregulation, and ■ indicating upregulation. (**b,e,h**) Principal component analysis plots of total identified proteins. The plots show separation between samples according to groups based on protein expression profiles: (**b**) Cells cultured at 5 kPa vs. 18 kPa. **e**) Cells cultured at 5 kPa vs. 5 kPa + SFN. (**h**) Cells cultured at 18 kPa vs. 18 kPa + SFN. The X and Y axes represent principal components 1 and 2, respectively. Prediction ellipses indicate the 95% confidence interval for each group. (**c,f,i**) Volcano plot illustrating total identified proteins for each group comparison: (**c**) 5 kPa vs. 18 kPa, (**f**) 5 kPa vs. 5 kPa + SFN, **i**) 18 vs. 18 kPa + SFN. Upregulated DEPs ●, downregulated ●, while non significantly expressed proteins are shown as ●.

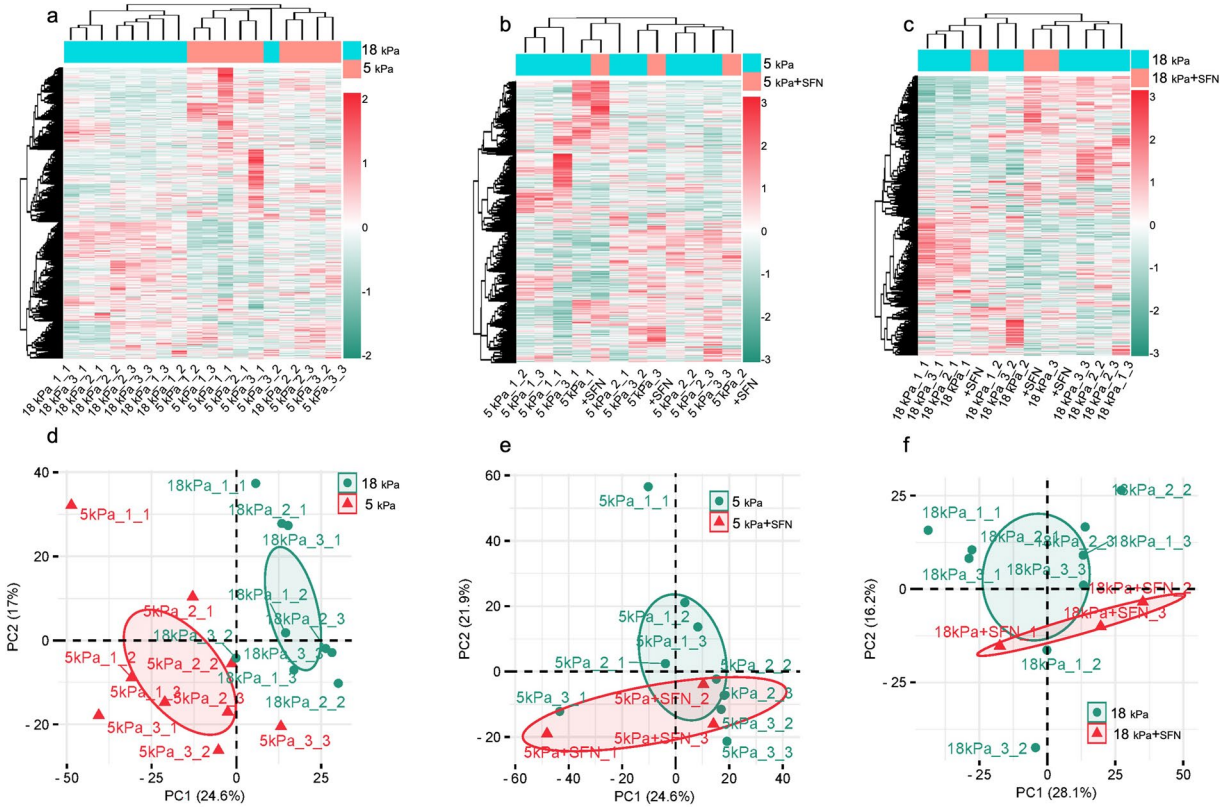

Fig. 4 Non-Averaged Differential Protein Expression Analysis of hCMEC/D3 Cells under Different Conditions. (**a,b,c**) Hierarchical clustering heatmap analysis of total identified proteins, highlighting sample clustering based on sample group: (**a**) 5 kPa vs. 18 kPa, (**b**) 5 kPa vs. 5 kPa + SFN, (**c**) 18 vs. 18 kPa + SFN. The color bars represent downregulated ■, and upregulated ■ protein expressions. (**d,e,f**) Principal component analysis plots of total identified proteins showing sample separation based on sample group: (**d**) 5 kPa vs. 18 kPa, (**e**) 5 kPa vs. 5 kPa + SFN, (**f**) 18 vs. 18 kPa + SFN. X and Y axes denote principal component 1 and principal component 2, respectively. Prediction ellipses indicate that, with a 95% probability, a new observation from the same group will fall within the ellipse. Samples are labeled with the first number indicating the number of biological replicate and the second indicating the number of technical replicates for each condition (See Table 1 for details).

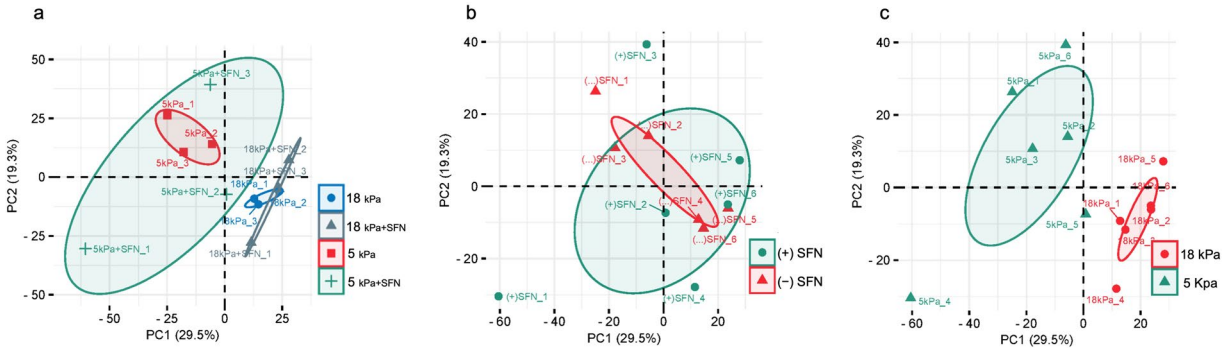

Fig. 5 Comparative Effects of Oxygen Levels and SFN Treatment on Sample Separation. Principal component analysis plots of total identified proteins, showing sample separation between comparison groups based on: (**a**) Oxygen level and/or SFN treatment, (**b**) SFN treatment only, (**c**) Oxygen levels only. X and Y axes denote principal component 1 and principal component 2, respectively. Prediction ellipses indicate that, with 95% probability, a new observation from the same group will fall within the ellipse.

Mass spectrometry downstream data analysis. Multivariate statistical analyses, including Hierarchical Clustering Analysis (HCA) and Principal Component Analysis (PCA), were performed on the entire set of identified proteins to explore differential expression patterns. Input files consisted of lists of identified proteins along with their respective normalized expression values. All analyses were conducted using the SRplot web tool[29]

(https://www.bioinformatics.com.cn/srplot). For HCA, data were scaled by rows, and a bidirectional clustering approach was applied. Pearson correlation was selected as the distance metric, and average linkage was used as the clustering method. In PCA, data centering and scaling were applied by default, with confidence ellipses included to highlight group separation. Finally, volcano plots were generated in an SRplot to visualize differential expression patterns of the identified proteins highlighting upregulated and downregulated DEPs (significance < 0.05, $|\text{fold change}| \geq 1.4$).

HCA of cells adapted to 18 kPa versus those adapted to 5 kPa O_2 revealed clear segregation of samples based on oxygen levels (Fig. 3a), underscoring the substantial impact of oxygen tension on the cellular proteome. Consistent with these findings, PCA also demonstrated distinct grouping according to the oxygen conditions (Fig. 3b). In contrast, no clear separation was observed between cells cultured at 5 kPa with sulforaphane (SFN) treatment compared to controls (Fig. 3d,e). However, clear separation was evident in both HCA and PCA when cells were cultured at 18 kPa (Fig. 3g,h). These results indicate that SFN has minimal effects on cells adapted to 5 kPa oxygen but induces substantial proteomic changes at 18 kPa oxygen. Further insights were gained from examining DEPs in the volcano plot analysis as follows: in the 18 vs. 5 kPa comparison, 91 proteins were upregulated and 61 were downregulated (Fig. 3c). For the 5 kPa vs. 5 kPa + SFN comparison, only 17 proteins were upregulated and 3 downregulated (Fig. 3f). In contrast, the 18 kPa vs. 18 kPa + SFN comparison revealed 14 upregulated and 8 downregulated proteins (Fig. 3i). Additional details are provided in Fig. 4, which presents similar findings for samples without averaging technical replicates, offering a higher resolution of individual sample clustering. The HCA and PCA plots in non-averaged form demonstrate consistent trends regarding sample grouping based on oxygen tension and SFN treatment, further validating the robustness of the observed patterns. Collectively, these results suggest that oxygen tension is the dominant factor driving sample segregation, as evident from the clear separation of groups in both averaged and non-averaged analyses. SFN treatment, in contrast, exerts a more subtle effect, with a noticeable impact observed only under 18 kPa oxygen conditions, as highlighted in Fig. 5. This indicates that the influence of SFN is strongly dependent on pericellular/intracellular oxygen levels and is more pronounced under 18 kPa O_2 levels, highlighting a clear interplay between oxygen tension and SFN treatment in shaping the proteomic profile and impacting research outcomes.

Code availability

The Methods section contains a detailed description of the performed data analysis. No custom code was utilized in this study for the analysis of the presented data.

Received: 18 February 2025; Accepted: 9 May 2025;
Published online: 12 June 2025

References

1. Keeley, T. P. & Mann, G. E. Defining Physiological Normoxia for Improved Translation of Cell Physiology to Animal Models and Humans. *Physiol Rev* **99**, 161–234 (2019).
2. Beumer-Chuwonpad, A. *et al*. Memory CD8+ T cells upregulate glycolysis and effector functions under limiting oxygen conditions. *Eur J Immunol* **53**, e2249918 (2023).
3. Fernandez, E. *et al*. Transcriptomic and metabolic signatures of neural cells cultured under a physiologic-like environment. *Journal of Biological Chemistry* **300**, 107937 (2024).
4. Adebayo, A. K. *et al*. Oxygen tension-dependent variability in the cancer cell kinome impacts signaling pathways and response to targeted therapies. *iScience* **27**, 110068 (2024).
5. Timpano, S. & Uniacke, J. Human cells cultured under physiological oxygen utilize two cap-binding proteins to recruit distinct mRNAs for translation. *Journal of Biological Chemistry* **291**, 10772–10782 (2016).
6. Halliwell, B. Oxidative stress in cell culture: An under-appreciated problem? *FEBS Lett* **540**, 3–6 (2003).
7. Tiboldi, A. *et al*. Oxygen-Dependent Changes in the N-Glycome of Murine Pulmonary Endothelial Cells. *Antioxidants* **10**, 1947 (2021).
8. Ostergaard, L. *et al*. Proteomics reveals lowering oxygen alters cytoskeletal and endoplasmatic stress proteins in human endothelial cells. *Proteomics* **9**, 4457–67 (2009).
9. Cater, D. B., Garattini, S., Marina, F. & Silver, I. A. Changes of oxygen tension in brain and somatic tissues induced by vasodilator and vasoconstrictor drugs. *Proc R Soc Lond B Biol Sci* **155**, 136–157 (1961).
10. Sweeney, M. D., Sagare, A. P. & Zlokovic, B. V. Blood-brain barrier breakdown in Alzheimer disease and other neurodegenerative disorders. *Nat Rev Neurol* **14**, 133–150 (2018).
11. Smith, M. J. *et al*. Redox and metal profiles in human coronary endothelial and smooth muscle cells under hyperoxia, physiological normoxia and hypoxia: Effects of NRF2 signaling on intracellular zinc. *Redox Biol* **62**, 102712 (2023).
12. Warpsinski, G. *et al*. Nrf2-regulated redox signaling in brain endothelial cells adapted to physiological oxygen levels: Consequences for sulforaphane mediated protection against hypoxia-reoxygenation. *Redox Biol* **37**, 101708 (2020).
13. Altun, H. Y. *et al*. Visualizing hydrogen peroxide and nitric oxide dynamics in endothelial cells using multispectral imaging under controlled oxygen conditions. *Free Radic Biol Med* **221**, 89–97 (2024).
14. Miri, S. M. *et al*. Development of an Oxygen-Insensitive Nrf2 Reporter Reveals Redox Regulation under Physiological Normoxia. *ACS Sens* https://doi.org/10.1021/acssensors.4c03167 (2025).
15. Sevimli, G. *et al*. Nitric oxide biosensor uncovers diminished ferrous iron-dependency of cultured cells adapted to physiological oxygen levels. *Redox Biol* **53**, 102319 (2022).
16. Ji, Y. *et al*. Integrated transcriptomic and proteomic profiling reveals the key molecular signatures of brain endothelial reperfusion injury. *CNS Neurosci Ther* **30**, e14483 (2024).
17. Yamamoto, M., Kensler, T. W. & Motohashi, H. The KEAP1-NRF2 System: a Thiol-Based Sensor-Effector Apparatus for Maintaining Redox Homeostasis. *Physiol Rev* **98**, 1169–1203 (2018).
18. Chapple, S. J. *et al*. Bach1 differentially regulates distinct Nrf2-dependent genes in human venous and coronary artery endothelial cells adapted to physiological oxygen levels. *Free Radic Biol Med* **92**, 152–162 (2016).
19. Poller, B. *et al*. The human brain endothelial cell line hCMEC/D3 as a human blood-brain barrier model for drug transport studies. *J Neurochem* **107**, 1358–1368 (2008).
20. Tai, L. M. *et al*. Polarized P-glycoprotein expression by the immortalised human brain endothelial cell line, hCMEC/D3, restricts apical-to-basolateral permeability to rhodamine 123. *Brain Res* **1292**, 14–24 (2009).

21. Wiśniewski, J. R., Zougman, A., Nagaraj, N. & Mann, M. Universal sample preparation method for proteome analysis. *Nat Methods* **6**, 359–362 (2009).
22. Barakat, S. *et al*. Bioenergetic shift and proteomic signature induced by lentiviral-transduction of GFP-based biosensors. *Redox Biol* **78**, 103416 (2024).
23. Okuda, S. *et al*. JPOSTrepo: An international standard data repository for proteomes. *Nucleic Acids Res* **45**, D1107–D1111 (2017).
24. Barakat, S. & Eroğlu, E. Impact of Oxygen Tension on the Proteomic Profile of hCMEC/D3 Cells and Implications for Drug Screening. *jPOST* https://repository.jpostdb.org/entry/JPST003477.0 (2025).
25. Deutsch, E. W. *et al*. The ProteomeXchange consortium at 10 years: 2023 update. *Nucleic Acids Res* **51**, D1539–D1548 (2023).
26. Barakat, S. & Eroğlu, E. Impact of Oxygen Tension on the Proteomic Profile of hCMEC/D3 Cells and Implications for Drug Screening. *ProteomeXchange* http://identifiers.org/px:PXD060622 (2025).
27. Alonso, R. *et al*. Babelomics 5.0: functional interpretation for new generations of genomic data. *Nucleic Acids Res* **43**, W117–W121 (2015).
28. Medina, I. *et al*. Babelomics: an integrative platform for the analysis of transcriptomics, proteomics and genomic data with advanced functional profiling. *Nucleic Acids Res* **38**, W210–3 (2010).
29. Tang, D. *et al*. SRplot: A free online platform for data visualization and graphing. *PLoS One* **18**, e0294236 (2023).

Acknowledgements

We gratefully acknowledge the support of the European Molecular Biology Organization (EMBO, IG 4113 to E.E.), British Heart Foundation (PG/24/11598 to G.E.M.), and the Scientific and Technological Research Council of Turkey (TÜBITAK, 123C217 to E.E). We thank Dr. Richard Siow from King's College London for providing hCMEC/D3 cells.

Author contributions

S.B. contributed to proteomic data generation and analysis. F.Y. conducted the hCMEC/D3 experiments and sample preparation for proteomic analysis. H.E.Y. assisted in proteomics data generation. K.K. contributed to data analysis. The senior authors G.E.M. and E.E. provided conceptualization and supervision of the study and secured external funding for the project. All authors contributed to drafting the manuscript and approved it.

Competing interests

The authors declare no competing interests.

Additional information

Correspondence and requests for materials should be addressed to S.B. or K.K.